Clays and Clay Minerals, Vol. 32, No. 2, 81–92, 1984.

REVIEW OF CATION ORDERING IN MICAS

S. W. BAILEY

Department of Geology and Geophysics, University of Wisconsin–Madison
Madison, Wisconsin 53706

Abstract—Long-range ordering of tetrahedral cations in micas is favored by phengitic compositions, by the $3T$ stacking sequence of layers, and by tetrahedral Si:Al ratios near 1:1. Phengites of the $1M$, $2M_1$, and $2M_2$ polytypes are said to show partial ordering of tetrahedral cations, although the amounts of tetrahedral substitutions are small and the accuracies of determination are not as large as desired. The $3T$ structures of muscovite, paragonite, lepidolite, and protolithionite show tetrahedral ordering, as do the $2M_1$ brittle micas margarite and an intermediate between margarite and bityite. Muscovite-$3T$ and margarite-$2M_1$ are also slightly phengitic relative to their ideal compositions. Examples of octahedral cation ordering in micas are more abundant and are to be expected when cations of different size and charge are present. Octahedron M(1) with its OH,F groups in the *trans* orientation tends to be larger than the mean of the two *cis* octahedra as a result of the ordering of cations and vacancies. In some samples ordering has reduced the true symmetry to a subgroup of that of the ideal space group. If ordering in subgroup symmetry results in ordered patterns of different geometries but similar energies in very small domains, the average over all unit cells may simulate long-range disorder.

Key Words—Cation ordering, Lepidolite, Margarite, Mica, Muscovite, Paragonite, Phengite.

INTRODUCTION

Where ionic substitutions occur in a mica the possibility exists that the different cations that occupy a given type of structural site may do so in either a regular or irregular manner. A truly random distribution over many unit cells is required to meet the definition of substitutional solid solution in which, on the average, each cation site in the unit cell is represented by a hybrid atom that is statistically part atom A, part atom B, etc. This is the disordered state. But there may be a tendency instead for complete or partial ordering of the constituent cations over the available positions as a result of size and/or bonding differences of the cations involved or of some inherent structural difference between the positions. The presence or absence of such ordering is important in evaluating the overall energy and stability of these structures.

One of the problems in studying ordering in layer silicates is that the ideal space-group symmetry that is conferred by a particular stacking sequence of layers with disordered cation distributions may not be the true resultant symmetry. The pattern of cation ordering that has been adopted may lower the true symmetry relative to that of the disordered state. For example, the symmetries of the ideal space groups require all interlayer cations to be equivalent (i.e., disordered) for all six standard mica polytypes of Smith and Yoder (1956) and the tetrahedral cations to be equivalent for the $1M$, $2Or$, and $6H$ micas. Any ordering that takes place for these cations necessarily lowers the symmetry to a subgroup of that of the disordered state. The lower subgroup symmetry may be very difficult to detect in view of the large influence of the stacking sequence of layers on the diffraction intensities, an unfortunate consequence of a high degree of pseudosymmetry. The ordering must be investigated in each possible subgroup symmetry by some method that negates the pseudosymmetry.

LONG-RANGE ORDERING

Bailey (1975) summarized the results of detection of cation ordering in layer silicates in both ideal and subgroup symmetries. The results of tetrahedral and octahedral ordering for the micas have been updated and are shown here as Tables 1 and 3. No ordering of interlayer cations has been reported.

Ordering of tetrahedral cations

Ordering of tetrahedral cations is relatively rare in micas. About 70 refinements of mica structures have been reported, but only ten examples of ordering of tetrahedral Si,Al merit consideration here. One of the major mysteries regarding micas is why the most common species are disordered (namely muscovite-$2M_1$, phlogopite-$1M$, and biotite-$1M$), even though these species may occur in their host rocks immediately adjacent to other silicates that are completely ordered, such as maximum microcline and low albite.

In Table 1 only those specimens are listed for which the authors have stated that tetrahedral cation ordering occurs and on which reasonable structural refinement has been performed. Less certain examples are not listed. Even in these best examples the final residual values (R) between observed and calculated spectral amplitudes and the deviations between analyzed and calculated tetrahedral compositions are not as small as desired for some specimens. Assuming the validity of these examples, however, the obvious trends emerge

Table 1. Examples of tetrahedral cation ordering in micas.

Reference	Species	Space group	Number of refl.	Final R (%)	Mean T–O (Å)	Tet. comp. from Eq.[1]	Total Al^{IV} From Eq.[1]	Total Al^{IV} From anal.
Güven and Burnham (1967)	muscovite-3*T* (Sultan Basin, Washington)	$P3_112$	280	2.4	T(1) = 1.670 T(2) = 1.603	$Si_{0.62}Al_{0.38}$ $Si_{1.0}$	0.76	0.89
Güven (1971a)	phengite-2M_1 (Tiburon peninsula, California)	*C*2/*c*	557	4.5	T(1) = 1.621 T(2) = 1.633	$Si_{0.92}Al_{0.08}$ $Si_{0.85}Al_{0.15}$	0.46	0.61
Zhoukhlistov *et al.* (1973)	phengite-2M_2 (N. Armenia)	*C*2/*c*	504	11.7	T(1) = 1.619 T(2) = 1.653	$Si_{0.93}Al_{0.07}$ $Si_{0.72}Al_{0.28}$	0.70	0.50
Sidorenko *et al.* (1975)	phengite-1*M* (Transbaikal, U.S.S.R.)	*C*2	588	10.9	T(1) = 1.614 T(2) = 1.633	$Si_{0.96}Al_{0.04}$ $Si_{0.85}Al_{0.15}$	0.38	0.49
Guggenheim and Bailey (1977)	zinnwaldite-1*M* (Erzgebirge, D.D.R.)	*C*2	1493	5.7	T(1) = 1.646 T(2) = 1.639	$Si_{0.77}Al_{0.23}$ $Si_{0.81}Al_{0.19}$	0.84	0.91
Sidorenko *et al.* (1977)	paragonite-3*T* (locality ?)	$P3_112$	208	13.0	T(1) = 1.609 T(2) = 1.684	$Si_{0.99}Al_{0.01}$ $Si_{0.53}Al_{0.47}$	0.96	1.04
Brown (1978)	lepidolite-3*T* (Kalgoorlie, Australia)	$P3_112$	705	4.7	T(1) = 1.652 T(2) = 1.617	$Si_{0.73}Al_{0.27}$ $Si_{0.94}Al_{0.06}$	0.66	0.52
Guggenheim and Bailey (1975, 1978)	margarite-2M_1 (Chester, Pennsylvania)	*Cc*	1071	4.0	T(1) = 1.747 T(2) = 1.633 T(22) = 1.736 T(11) = 1.623	$Si_{0.15}Al_{0.85}$ $Si_{0.85}Al_{0.15}$ $Si_{0.21}Al_{0.79}$ $Si_{0.91}Al_{0.09}$	1.88	1.89
Pavlishin *et al.* (1981)	protolithionite-3*T* (Ukraine, U.S.S.R.)	$P3_112$	702	4.7	T(1) = 1.665 T(2) = 1.633	$Si_{0.65}Al_{0.35}$ $Si_{0.85}Al_{0.15}$	1.00	1.13
Lin and Guggenheim (1983)	intermediate margarite-bityite-2M_1 (Zimbabwe)	*Cc*	1927	3.0	T(1) = 1.723 T(2) = 1.628 T(22) = 1.721 T(11) = 1.632	(Be^{IV} also present)		

[1] Indicated Si, Al and Al^{IV} contents are as given by the regression equation of Hazen and Burnham (1973).

that tetrahedral ordering is favored in the 3*T* structure, for phengitic compositions, and for Si:Al^{IV} ratios near 1:1. The 3*T* structures of muscovite, paragonite, lepidolite, and protolithionite all have been stated to be ordered, as have phengites in the 1*M*, 2M_1, and 2M_2 stacking arrangements. Muscovite-3*T* is slightly phengitic also. Sidorenko *et al.* (1975) commented that the correlation between phengitic composition and ordering is probably not coincidental. In contrast to the order found in dioctahedral phengite-2M_2, three determinations of the structure of the trioctahedral lepidolite-2M_2 detected no tetrahedral ordering. No significant tetrahedral ordering has been found for any of the abundant trioctahedral 1*M* micas, although the possibility of ordering to subgroup symmetry has seldom been investigated. Because of similarity in their scattering powers, ordered patterns of Si and Al in these studies have been detected by the differences noted in the mean T–O bond lengths between nonequivalent tetrahedra. Hazen and Burnham (1973) found a linear regression relation T–O = 1.608 Å + 0.163[$x_{Al}/(x_{Al} + x_{Si})$] for the mean tetrahedral bond lengths in the micas; this equation is used in Table 1 to calculate the tetrahedral compositions. Alternation of the smaller Si and the larger Al around the six-fold tetrahedral rings has been the only ordering pattern thus far found in micas.

Although muscovite-2M_1 has two independent tetrahedra in its ideal symmetry, all well-refined structures show relatively small differences in the mean T–O bond lengths of the two tetrahedra. In discussing the relationship between the disordered 2M_1 and the ordered 3*T* forms of muscovite, Güven (1971b) pointed out that the two tetrahedral sheets within a single mica layer are related to each other by a center of symmetry in the disordered 2M_1 structure but by a lateral twofold rotation axis in the ordered 3*T* structure. An apical oxygen attached to one Si^{4+} tetrahedral cation and to two Al^{3+} octahedral cations has its negative charge exactly balanced, but an excess negative charge exists if

Al^{3+} substitutes for Si^{4+}. Güven pointed out that if tetrahedral cation ordering were present in the $2M_1$ structure, two apical oxygens would be present with unsatisfied negative charges arrayed along a diagonal octahedral edge that is shared between two Al octahedral cations. Such an arrangement maintains the inversion center that lies on the shared edge, but is potentially unstable because the shortening of shared edges inherent in these dioctahedral sheets will lead to repulsion between apical oxygens with excess negative charges. In the ordered $3T$ structure the octahedral edge in question lies between one occupied and one vacant octahedral site so that edge-shortening is not required.

It is also possible to describe an ordered $2M_1$ structure in subgroup *Cc* so that compositionally similar tetrahedra of adjacent sheets are not related by the inversion center but instead by a lateral two-fold rotation axis that does not hold for the structure as a whole. This latter ordered structure has been found in the $2M_1$ brittle mica margarite (Guggenheim and Bailey, 1975, 1978) and in a specimen that is chemically intermediate between margarite and bityite (Lin and Guggenheim, 1983). The *Cc* subgroup structure should be especially favorable because it allows complete ordering of the four tetrahedral cations into four nonequivalent sites (in contrast to two sites in *C*2/*c*). Nevertheless, the greater driving force for ordering inherent in these brittle micas due to their greater tetrahedral substitutions (2Si + 2Al in margarite and 2Si + 2Al,Be in bityite) is required to realize the ordering, because the ordering pattern is not adopted by either muscovite-$2M_1$ (Guggenheim and Bailey, 1975) or paragonite-$2M_1$ (Lin and Bailey, 1984) that have tetrahedral compositions of 3Si + 1Al.

The structures listed in Table 1 have been derived by both X-ray diffraction and electron diffraction methods and represent differing degrees of accuracy. The quality of the data as compared to the structural model can be judged by the final agreement between observed and calculated spectral amplitudes (R values) and by the degree of agreement between the total Al^{IV} contents as determined by the size differences of the tetrahedra and by chemical analysis (Table 1). The significance of the tetrahedral size differences also can be judged statistically by consideration of the determinative errors involved. If σ_l is the error (standard deviation) of an individual bond length, the error of the mean of n values is $\sigma_n = \sigma_l/n^{1/2}$, where $n = 4$ for a tetrahedron. For the difference Δ between the two mean values of the same accuracy $\sigma_\Delta = 2^{1/2}\sigma_n$ and in order for an observed difference Δ to be statistically significant at the 1% level, it should be equal to or greater than $2.33\sigma_\Delta$ or at the 0.1% highly significant level should be equal to or greater than $3.09\sigma_\Delta$ according to the criteria of Cruickshank (1949). Because of the difficulty in deriving true values of the determinative errors, many crystallographers prefer an observed bond length difference to be at least 3.0 standard deviations, rather than 2.33, for significance at the 1% level. Significance at the 1% level as used here means that there is a 1% probability that by chance a bond length A could be observed as greater than bond length B by at least Δ, although really equal to B. In this review bond-length differences between $2.3\sigma_\Delta$ and $3.1\sigma_\Delta$ are treated as being in the borderline area of significance at this level. Table 2 lists the results of the application of this statistical approach to the structures of Table 1. Published σ_l or σ_n values have been used for all samples except for phengite-$2M_2$, where the published errors in atomic coordinates have been averaged for each atom in order to calculate the standard deviations of the bond lengths.

Table 2. Statistical analysis of tetrahedral size differences.

Polytype	Species	σ_n (Å)	σ_Δ (Å)	Δ (Å)	Δ/σ_Δ
$1M$	phengite	0.009	0.0127	0.019	1.5
	zinnwaldite	0.002	0.0028	0.007	2.5
$2M_1$	phengite	0.003	0.0042	0.012	2.9
	margarite	0.0035	0.0049	0.1135	23.2
	margarite-bityite	0.003	0.0042	0.092	21.9
$2M_2$	phengite	0.005	0.0071	0.034	4.8
$3T$	muscovite	0.0085	0.0120	0.067	5.6
	paragonite	0.020	0.0283	0.075	2.7
	lepidolite	0.008	0.0113	0.035	3.1
	protolithionite	0.005	0.0071	0.032	4.5

According to the results in Table 2 the differences between the tetrahedral bond lengths are highly significant for margarite-$2M_1$, margarite-bityite-$2M_1$, muscovite-$3T$, phengite-$2M_2$, and protolithionite-$3T$ (Δ/σ_Δ = 23.2 to 4.5). The difference in phengite-$1M$ is not statistically significant at the 1% level (Δ/σ_Δ = 1.5). All of the other structures group together in the borderline range with Δ/σ_Δ values between 2.5 and 3.1. The reasons for the lower significance levels in this latter group are different for different specimens. For paragonite-$3T$ it is due to the larger determinative error σ_n; for phengite-$2M_1$ and lepidolite-$3T$, where the errors are smaller, it appears to be due to a combination of a small amount of tetrahedral substitution and incomplete ordering; and for zinnwaldite-$1M$, to a small degree of ordering. Clearly, only a small number of refinements of high accuracy have detected any substantial degree of tetrahedral ordering in micas. Ordering of tetrahedral Si,Fe^{3+} has been verified in subgroup symmetry in anandite-$2O$ (Filut and Bailey, in preparation), but is not considered here.

Ordering of octahedral cations

Octahedral cation ordering, as judged either by observed differences in mean M–O,OH,F bond lengths or by refinement of octahedral occupancies based on differences in scattering powers of the cations, is more

https://doi.org/10.1346/CCMN.1984.0320201 Published online by Cambridge University Press

common than tetrahedral ordering in micas. Table 3 gives the bond lengths and reported octahedral compositions for the best documented examples of octahedral ordering in the micas. Note in some cases that verification of ordering depends entirely on refinement of the octahedral occupancies because the mean bond lengths of all of the octahedra are similar. Statistical analysis of the bond lengths is not helpful in such cases. It should be noted also that many specimens selected for structural refinement have been end-member compositions with only one element present in octahedral coordination. Although ordering between Mg and Fe^{2+} is uncommon, Table 3 shows that ordering is common between other octahedral cations of different sizes and charges. It may be concluded that ordering is to be expected if the octahedral compositions are conducive.

In all dioctahedral micas the vacant octahedral site has been found to be located on the mirror plane of each 2:1 layer, i.e., in site M(1) that has its OH,F groups on opposite octahedral corners in the *trans* orientation. This arrangement can be considered as a form of ordering and is in accord with the pattern of ordering usually found in trioctahedral micas: the *trans* octahedron M(1) tends to be larger than the mean of the M(2) octahedra, which have their OH,F groups on adjacent corners in the *cis* orientation. An exception to this generalization was previously believed to be the structure of the brittle mica clintonite-1*M* (xanthophyllite) for which Takéuchi and Sadanaga (1966) found the smaller Al in the M(1) and the larger Mg in the M(2) sites. A redetermination of the structure by neutron diffraction (W. Joswig, University of Frankfurt, Frankfurt-am-Main, Germany, personal communication, 1983), however, shows that one Mg is in M(1) and that the other Mg plus the Al are disordered over the two M(2) sites. Levillain *et al.* (1981) cited Mössbauer data to suggest that a similar octahedral ordering pattern exists in the structure of a synthetic siderophyllite of composition $K(Fe^{2+}{}_2Al)(Si_2Al_2)O_{10}(OH)_2$.

The relative ratio of large to small octahedra, however, is not always in accord with the ratio of large to small octahedral cations present. For example, in synthetic lepidolite-1*M* of the polylithionite composition (Takeda and Burnham, 1969) two large octahedral Li ions and one smaller Al ion are present by chemical analysis. Yet the ordering pattern creates only one large octahedral site at M(1) on the mirror plane but two smaller symmetry-related M(2) sites. The compositions inferred from the refinement of scattering powers in these sites are $M(1) = Li_{0.89}Al_{0.11}$ and $M(2) = (Li_{0.55}Al_{0.45}) \times 2$. Similar ordering patterns have been observed in both the 1*M* and $2M_2$ forms of natural lepidolites from Elba, Italy, and Radkovice, Czechoslovakia (Table 3).

Hybrid atoms, such as those cited above that are part atom A and part atom B, are a statistical device to indicate disorder of those atoms in a given site when averaged over many unit cells. The atoms obviously cannot exist as hybrids in the structure, and especially near critical compositions such as $(Li_{0.5}Al_{0.5}) \times 2$ one might suspect that ordering within the M(2) octahedra has taken place to lower the symmetry or to create a superlattice. Guggenheim and Bailey (1977) investigated this possibility for a zinnwaldite-1*M* crystal from the Erzgebirge. They found that despite lack of appreciable tetrahedral ordering, octahedral ordering has lowered the resultant symmetry from the ideal *C*2/*m* symmetry to that of subgroup *C*2 with all three octahedra having different scattering powers. All of the octahedral Al is concentrated in one of the M(2) sites, and the remaining Fe, Li and other cations are distributed not quite equally over M(1) and the second M(2) site. The hybrid F,OH atom has moved off the mirror plane of the 1*M* structure in order to coordinate more closely with the small Al. The ideal space group of lepidolite-3*T* permits all three octahedra to be of different composition, and the structure by Brown (1978) shows this to be the case for a crystal from Australia. Guggenheim (1981) found variable amounts and patterns of octahedral ordering in different 1*M* lepidolite crystals, some in ideal symmetry and some in subgroup symmetry. This arrangement illustrates the dangers inherent in making generalizations or extrapolations based on the structural refinement of a single specimen.

Toraya (1981) noted that the *trans* M(1) site in 1*M* micas not only tends to be larger than M(2), but also to be occupied by a cation of lower charge or by a vacancy. He explained that in the reverse situation an increase in size of M(2) would stretch the O–O edge that is shared between two adjacent M(2) cations (thus increasing repulsion between the cations), shrink the O–OH,F edge shared between M(1) and M(2) (decreasing repulsion), and increase repulsion between oxygens on unshared lateral edges of M(1) due to its smaller size. An increase in size of M(1), however, gives the reverse effect on all of these edges and is energetically more favorable overall. The only unfavorable factor would be increased repulsion between M(1) and M(2) across the shared O–OH,F edge, and this is minimized by having a low charge on the M(1) cation.

Several micas have been described with total octahedral occupancies halfway between dioctahedral and trioctahedral. Levinson (1953) showed in the muscovite-lepidolite series that bulk compositions in this intermediate range actually are intimate mixtures of separate dioctahedral and trioctahedral phases. But in other series the intermediate compositions appear to apply to a single phase, and it is of interest to know the nature of the structural adaptations.

Toraya *et al.* (1976, 1978) refined the structures of two synthetic micas having octahedral occupancies close to $Mg_{2.5}\square_{0.5}$. In the silicate mica $[\sim K_{0.88}(Mg_{2.56}\square_{0.44})Si_4O_{10}F_2]$ the vacancies were found to be distributed

Table 3. Examples of octahedral cation ordering in micas.

Reference	Species	Space group	Number of reflections	Final R (%)	Mean M–O,OH (Å)	Octahedral composition[1]
Takéuchi and Sadanaga (1966)	clintonite-1*M* (Chichibu mine, Japan)	*C*2/*m*	384	10.4	M(1) = 2.019 M(2) = 2.050 × 2	$Al_{0.72}Mg_{0.18}\square_{0.10}$ $Mg_{1.0}$ × 2
Güven and Burnham (1967)	muscovite-3*T* (Sultan Basin, Washington)	$P3_112$	280	2.4	M(2) = 1.973 M(3) = 1.913	$Al_{0.83}Mg_{0.08}Fe^*_{0.09}$ $Al_{1.0}$
Takeda and Burnham (1969)	synthetic lepidolite-1*M*	*C*2/*m*	328	5.1	M(1) = 2.106 M(2) = 1.981 × 2	$Li_{0.89}Al_{0.11}$ $Li_{0.55}Al_{0.45}$
Takeda *et al.* (1971)	lepidolite-2M_2 (Rozna, Czechoslovakia	*C*2/*c*	471	7.2	M(1) = 2.144 M(2) = 1.967 × 2	$Li_{0.35}Al_{0.10}\square_{0.55}$ $Li_{0.35}Al_{0.65}$
Sartori *et al.* (1973)	lepidolite-2M_2 (Elba, Italy)	*C*2/*c*	525	9.6	M(1) = 2.123 M(2) = 1.980 × 2	$Li_{0.95}Al_{0.05}$ $Li_{0.37}Al_{0.63}$
Sidorenko *et al.* (1975)	phengite-1*M* (Transbaikal, U.S.S.R.)	*C*2	588	10.9	M(2) = 1.920 M(3) = 1.957	$Al_{1.0}$ $Al_{0.8}Mg_{0.1}Fe^*_{0.1}$
Guggenheim and Bailey (1975, 1978)	margarite-2M_1 (Chester, Pennsylvania)	*Cc*	1071	3.0	M(2) = 1.903 M(3) = 1.915	$Al_{1.0}$ $Al_{0.96}Mg_{0.03}Fe^{2+}_{0.01}$
Sartori (1976)	lepidolite-1*M* (Elba, Italy)	*C*2/*m*	400	6.7	M(1) = 2.113 M(2) = 1.972 × 2	$Li_{0.95}Al_{0.05}$ $Li_{0.37}Al_{0.63}$
Guggenheim and Bailey (1977)	zinnwaldite-1*M* (Erzgebirge, D.D.R.)	*C*2	1493	5.7	M(1) = 2.132 M(2) = 1.882 M(3) = 2.131	$Fe^{2+}_{0.42}Li_{0.34}Fe^*_{0.10}\square_{0.14}$ $Al_{1.0}$ $Al_{0.05}Fe^{2+}_{0.36}Li_{0.33}Fe^*_{0.12}\square_{0.14}$
Sidorenko *et al.* (1977)	paragonite-3*T* (locality ?)	$P3_112$	208	13.0	M(1) = 2.061 M(2) = 1.965 M(3) = 1.981	$Al_{0.3}\square_{0.7}$ $Al_{0.9}\square_{0.1}$ $Al_{0.8}\square_{0.2}$
Toraya *et al.* (1977)	synthetic taeniolite-1*M*	*C*2/*m*	1303	2.4	M(1) = 2.058 M(2) = 2.061 × 2	$Mg_{0.71}Li_{0.29}$ $Mg_{0.66}Li_{0.34}$
Brown (1978)	lepidolite-3*T* (Kalgoorlie, Australia)	$P3_112$	705	4.7	M(1) = 2.036 M(2) = 2.113 M(3) = 1.920	$Li_{0.71}Al_{0.29}$ $Li_{0.96}R_{0.04}$ $Li_{0.18}Al_{0.82}$
Toraya *et al.* (1978)	synthetic 1*M* $K(Mg_{2.5}\square_{0.5})$ $Ge_4O_{10}F_2$ mica	*C*2/*m*	1413	5.5	M(1) = 2.178 M(2) = 2.070 × 2	$Mg_{0.60}\square_{0.40}$ $Mg_{0.95}\square_{0.05}$
Toraya *et al.* (1978)	synthetic Ge-taeniolite-1*M*	*C*2/*m*	1451	3.8	M(1) = 2.092 M(2) = 2.092 × 2	$Mg_{0.64}Li_{0.36}$ $Mg_{0.68}Li_{0.32}$
Swanson and Bailey (1981)	lepidolite-2M_1 (Biskupice, Czechoslovakia)	*C*2/*c*	971	9.1	M(1) = 2.107 M(2) = 1.977 × 2	$Li_{0.93}(Fe^*,Mg)_{0.07}$ $Li_{0.35}Al_{0.58}\square_{0.07}$
Guggenheim (1981)	lepidolite-1*M* (Radkovice, Czechoslovakia)	*C*2/*m*	1164	3.5	M(1) = 2.118 M(2) = 1.970 × 2	$Li_{0.91}Fe^*_{0.04}Mg_{0.05}$ $Li_{0.28}Al_{0.65}\square_{0.07}Fe^{3+}_{0.005}$
Guggenheim (1981)	lepidolite-1*M* (Tanakamiyama, Japan)	*C*2	807	6.2	M(1) = 2.120 M(2) = 1.878 M(3) = 2.126	$Li_{0.70}Al_{0.06}Fe^*_{0.06}\square_{0.18}$ $Al_{1.0}$ $Li_{0.71}Al_{0.07}Fe^*_{0.06}\square_{0.16}$
Guggenheim (1981)	lepidolite-2M_2 (Radkovice, Czechoslovakia)	*C*2/*c*	2764	4.8	M(1) = 2.121 M(2) = 1.966 × 2	$Li_{1.0}$ $Li_{0.24}Al_{0.65}(Mn,Mg,Fe^{3+})_{0.05}\square_{0.07}$
Pavlishin *et al.* (1981)	protolithionite-3*T* (Ukraine, U.S.S.R.)	$P3_112$	702	4.7	M(1) = 2.121 M(2) = 1.909 M(3) = 2.149	$Fe^{2+}_{0.53}Li_{0.26}Mg_{0.01}Fe^*_{0.06}\square_{0.14}$ $Al_{0.83}Fe^{3+}_{0.17}$ $Fe^{2+}_{0.53}Li_{0.26}Mg_{0.01}Fe^*_{0.06}\square_{0.14}$
Ohta *et al.* (1982)	oxybiotite-1*M* (Ruiz Peak, New Mexico)	*C*2/*m*	1125	5.0	M(1) = 2.077 M(2) = 2.059 × 2	$Mg_{0.62}Fe^*_{0.19}Al_{0.19}$ $Mg_{0.51}Fe^*_{0.29}Al_{0.03}Ti_{0.17}$
Ohta *et al.* (1982)	oxybiotite-2M_1 (Ruiz Peak, New Mexico)	*C*2/*c*	1676	4.5	M(1) = 2.076 M(2) = 2.060 × 2	$Mg_{0.61}Al_{0.19}Fe^*_{0.20}$ $Mg_{0.51}Al_{0.02}Fe^*_{0.30}Ti_{0.17}$

[1] Indicated octahedral compositions are as given by the authors. Fe* = Fe^{3+} + Fe^{2+} + Mn + Ti except where these elements are listed separately.

https://doi.org/10.1346/CCMN.1984.0320201 Published online by Cambridge University Press

equally over all three octahedral positions, thus structurally simulating a disordered trioctahedral mica. In the germanate mica $[K(Mg_{2.5}\square_{0.5})Ge_4O_{10}F_2]$ a greater concentration of vacancies was noted in the larger M(1) site, structurally simulating a true intermediate between dioctahedral and trioctahedral. For the latter material the authors postulated that M(1) needs to be expanded laterally by incorporating vacancies in order to fit better with the large Ge-rich tetrahedral sheet. Lin and Guggenheim (1983) reported a brittle mica intermediate between dioctahedral margarite-$2M_1$ and trioctahedral bityite-$2M_1$ that has an octahedral composition of $(Al_{2.044}Li_{0.547}Fe^{3+}_{0.007}\square_{0.402})$. Refinement of the structure in subgroup *Cc* indicates that two Al cations are concentrated in the M(2) and M(3) *cis* octahedra and that the larger *trans* M(1) octahedron contains primarily Li and vacancies. This distribution is also that of a true intermediate on average, but the authors cited the evidence of split hydrogen protons on electron density difference maps to emphasize that the crystal actually is composed of both dioctahedral (Li-poor) and trioctahedral (Li-rich) unit cells in which the orientations of the O..H vector are quite different. It is possible that cooperative forces would aggregate similar cells into two kinds of small domains that differ in their dioctahedral or trioctahedral nature, but the X-ray diffraction evidence is not definitive on the distribution of the unit cells. Another unusual octahedral ordering pattern involving an unequal distribution of cations and vacancies is that of a natural paragonite-$3T$ specimen in which the two octahedral Al cations are said to be distributed in differing amounts over all three independent octahedral positions. The normally vacant site M(1) actually has a composition of $Al_{0.3}\square_{0.7}$ according to electron density maps and analysis of the mean bond lengths derived from a high-voltage texture electron-diffraction study by Sidorenko *et al.* (1977), whereas M(2) = $Al_{0.9}\square_{0.1}$ and M(3) = $Al_{0.8}\square_{0.2}$.

Ordering of interlayer cations

Any ordering of interlayer cations necessarily reduces the symmetry to a subgroup of the parent space group for the six standard mica polytypes of Smith and Yoder (1956). No ordering of these cations has been reported, but the possibility does not appear to have been seriously investigated.

Unmixing of different size interlayer cations is well documented in the muscovite-paragonite-margarite ternary system. An especially interesting unmixing intergrowth also has been observed in the only known occurrence of wonesite. Veblen (1983) used transmission electron microscopy, electron diffraction, and X-ray analytical electron microscopy to show that wonesite having a bulk interlayer composition of $Na_{0.395}K_{0.073}Ca_{0.002}\square_{0.53}$ has exsolved into a very fine, lamellar intergrowth of talc and a wonesite of a different interlayer composition of approximately $Na_{0.505}K_{0.093}Ca_{0.002}\square_{0.40}$. The exsolved wonesite also is enriched in Al, Ti, Cr, and Fe relative to the exsolved talc. An asymmetric solvus is depicted as lying between talc (with no interlayer cations) and a hypothetical mica "E" (with no interlayer vacancies) that lies on the join between Na-phlogopite and preiswerkite. Surprisingly, the intergrown lamellae are inclined to (001) by an average angle of 37°.

Local charge balance

The stability of a structure would be enhanced if, in addition to the presence of tetrahedral and octahedral cation ordering, the ordered constituents can be arranged in patterns that provide charge balance between the local sources of excess positive and negative charges created by ordering. Local charge balance between the ordered constituents of tetrahedral and octahedral sheets has been recognized in certain specimens of chlorite and vermiculite. In these samples the local balance occurs as a result of a particular arrangement of an octahedral interlayer relative to the tetrahedral sheets of 2:1 layers above and below. In micas there is the added complication of a positively charged interlayer cation that cannot contribute to local charge balance because its charge necessarily is distributed equally over all of its basal oxygen neighbors. But local charge balance might still be possible within a 2:1 layer in two kinds of micas: (1) those that have a high amount of tetrahedral substitution of R^{3+} for R^{4+}, and for which part of the excess negative charge thus created on the tetrahedra is reduced by a positive charge due to octahedral substitution of R^{3+} for R^{2+} or R^{+} for $\square$, or (2) in trioctahedral micas of smaller tetrahedral substitution in which octahedral R^{3+} substitution in one site can be compensated in part by octahedral R^{1+} or vacancies in the other two sites. Logical candidates thus would include Al- or Fe^{3+}-rich biotites, lepidolite, zinnwaldite, masutomilite, wonesite, preiswerkite, and clintonite. It is of some interest to determine whether the concept of local charge balance has any validity in the micas.

Among the micas in Tables 1 and 3 for which both tetrahedral and octahedral cation ordering have been claimed, only in lepidolite-$3T$, protolithionite-$3T$, and zinnwaldite-$1M$ are there local sources of positive octahedral charge due to concentration of Al in one octahedral site. The geometric distribution of Al-rich octahedra (highest positive charges) and Al-rich tetrahedra (excess negative charges) in lepidolite-$3T$ and protolithionite-$3T$ does not lead to local charge balance. A different tetrahedral ordering pattern in zinnwaldite-$1M$, however, does create the correct geometry in which the underbonded apices of two Al-rich tetrahedra link to a diagonal shared edge of the Al-rich octahedron. Zinnwaldite-$1M$ is not the most desirable example to cite as proof of local charge balance, however, inas-

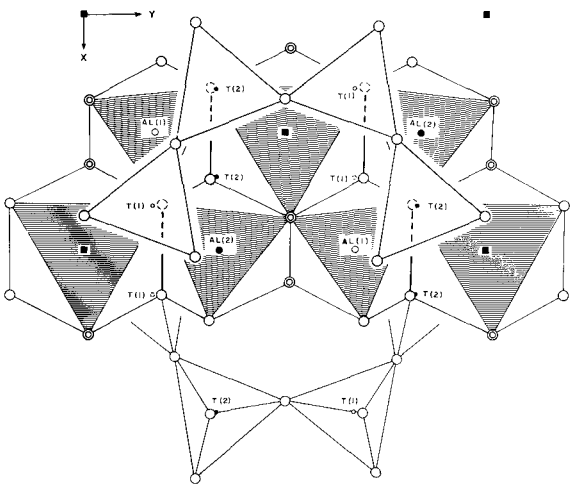

Figure 1. Portion of 2:1 layer of phengite-1*M* to illustrate separation of tetrahedral and octahedral sources of negative charge. The Al-substituted tetrahedra T(2) are linked by apical oxygens above and below to a diagonal edge (bold line) shared between an unsubstituted octahedron Al(1) and a vacant octahedron. The unsubstituted tetrahedra T(1) are linked to an edge shared between the Mg,Fe-substituted octahedron Al(2) and a vacant octahedron.

much as the degree of tetrahedral ordering is very small (Table 1).

Soboleva and Mineeva (1981) claimed the existence of a different type of charge balance in the structure of phengite-1*M* as determined by Sidorenko *et al.* (1975). Here, the substitution of tetrahedral Al^{3+} for Si^{4+} and of octahedral Mg^{2+} for Al^{3+} creates two different sources of negative charge, and the ordering places the local sources of the two negative charges as far apart as possible. This effect might better be termed avoidance of local charge imbalance. The geometry is illustrated in Figure 1. The Mg-substituted octahedron Al(2) has an overall negative charge because the nominal charges on the coordinating anions are greater than the positive bond strengths contributed to them by the enclosed hybrid cation. This octahedron is linked by a diagonal edge (bold line) to the O(1) apices of two of the most neutral tetrahedra (one Si-rich T(1) tetrahedron from each of the tetrahedral sheets within a 2:1 layer) while it is linked to the Al-substituted and negatively charged T(2) tetrahedra by two *trans* O(2) corners. The most neutral Al-rich octahedron Al(1), on the other hand, is linked most closely by the diagonal shared edge O(2)–O(2) to two of the Al-rich and negatively charged tetrahedra T(2) and by *trans* O(1) corners to the neutral T(1) tetrahedra.

For the 1*M* structure the type of charge balance illustrated in Figure 1 requires the substitution of lesser charged cations in both sheets (phengitic in this example) to permit the ordering and a reduced symmetry as a result of the ordering. It should be noted that the phengite-1*M* structure is not as accurately determined as desirable. The residual R value is 10.9%, and analysis of the determinative errors shows that, while the octahedral ordering is statistically significant (Δ mean M–O,OH = $4.4\sigma_\Delta$), the tetrahedral ordering is not, at the 1% level (Δ mean T–O = $1.5\sigma_\Delta$).

An infrared and cell-dimension study in the synthetic muscovite-celadonite system by Velde (1980) is of special interest here because of his interpretation that the data are consistent with octahedral ordering on the celadonite-1*M* side of the system at 10 kbar and by tetrahedral ordering at the muscovite side only at the higher pressure of 13 kbar. It is not known how the differences in distribution of vacancies over the three octahedral sites, as noted previously in paragonite-3*T*, would affect the infrared patterns or cell dimensions. The composition of the phengite-1*M* structure cited above places it at the midpoint of this series with respect to its tetrahedral Si:Al ratio of 3.51:0.49 although the octahedral R^{2+} substitution of 0.18 atoms is low and is correlated with a low interlayer cation total of 0.68 atoms. The phengite-1*M* structure indicates that the octahedral ordering is real and extends farther toward the muscovite end of the series in nature than indicated by Velde's data for the synthetic system. Velde's interpretation does not anticipate tetrahedral ordering for the composition of this specimen even at 13 kbar. Refinements of two other natural phengite specimens ($2M_2$ and $3T$) have indicated tetrahedral ordering without octahedral ordering (Tables 1 and 2), whereas for a third phengite ($2M_1$) neither tetrahedral nor octahedral ordering is indicated (Rule and Bailey, unpublished).

A better example of avoidance of local charge imbalance is provided by the structure of the brittle mica margarite-$2M_1$. The specimen studied by Guggenheim and Bailey (1975, 1978) also is slightly phengitic in that the tetrahedral Si:Al ratio of 2.11:1.89 has excess Si relative to the ideal 2:2 ratio, and this excess positive cationic charge is compensated by substitution of octahedral Mg and Fe^{2+} for Al. The pattern of tetrahedral and octahedral ordering adopted in subgroup *Cc* creates two local sources of excess negative charge that are separated as far as possible. Tetrahedral ordering is complete in this specimen, but the amount of octahedral substitution is small and the observed difference in mean octahedral bond lengths of 0.012 Å is only $2.7\sigma_\Delta$.

A questionable example of the same effect is found in the structure of paragonite-3*T* as a result of the postulated tetrahedral cation ordering and unequal distribution of cations and vacancies over the three octahedral sites. The statistical significance of the ordering again is borderline. The observed difference in mean T–O bond lengths of 0.075 Å is $2.7\sigma_\Delta$ (Table 2). The difference of 0.016 Å in the mean M–O,OH bond lengths

https://doi.org/10.1346/CCMN.1984.0320201 Published online by Cambridge University Press

of the two *cis* octahedra is not statistically significant ($\Delta = 0.8\sigma_\Delta$), but Sidorenko *et al.* (1977) stated that the inferred compositions of $Al_{0.9}\square_{0.1}$ and $Al_{0.8}\square_{0.2}$ for these octahedra along with $Al_{0.3}\square_{0.7}$ in M(1) gave the smallest R factor during refinement by successive Fourier syntheses (for which the determination errors are not known).

Thus, the available data do not prove any strong tendency for either local charge balance or avoidance of local charge imbalance as a result of cation ordering in micas. More accurate structural refinements are needed for cases such as those cited above where it is important to be able to determine the reality of ordering involving small amounts of substitution. But even if the small differences are real, Baur (1970) has shown that variations in bond lengths compensate adequately for most observed variations in valence saturations. The driving force for local charge balance in micas must, therefore, be minimal.

Standardized cation notation

More credence could be given to the significance of small bond length differences as a measure of ordering if they could be shown to be consistent for a given polytype, e.g., with T(1)–O > T(2)–O in all examples of ordering within the $2M_1$ structure, or to be in accord with established crystal chemical factors that might favor localization of a given cation in a specific tetrahedral or octahedral site. A standard notation for the possible sites is a necessary first step in investigating these possibilities, because to date different authors have used T(1), T(2), M(2), M(3), etc. as labels for different tetrahedral and octahedral sites and one cannot analyze Tables 1 and 3 in terms of an absolute locus of the ordered substitutions.

For the tetrahedral cations it is recommended that the first 2:1 layer of the structure be viewed parallel to the symmetry plane (real or pseudo) of the layer with the direction of the intralayer shift pointing away from the observer. The *trans* M(1) octahedron then will be located halfway between the edges of two hexagonal rings that differ by $a/3$ in projection onto (001), as in Figure 2. The tetrahedron in the upper tetrahedral sheet that is closest to M(1) and to the right of the symmetry plane is to be labeled T(1) and that to the left is T(2). In space group $C2/c$ for the $2M_1$ and $2M_2$ structures and in $P3_112$ for the $3T$ structure these tetrahedra are not equivalent by symmetry, and both must be used in the structural refinement. In $C2/m$, the ideal symmetry of the $1M$ structure, the two tetrahedra are equivalent and only T(1) need be used. In subgroup $C2$ the symmetry plane is lost and the two sites again are non-equivalent. The relationship of the upper tetrahedral sheet to the lower sheet and of the first 2:1 layer to successive layers is determined by the resultant symmetry, and the notation used for tetrahedra in these parts of the structure is immaterial for the present purpose. It is necessary to define what is meant by the "first layer" in multiple-layer structures, however, and this is done here by arbitrary reference to Figure 1.15 of Bailey (1980). The first layer in the $2M_1$ structure thus is defined as the one with its intralayer shift directed along the pseudohexagonal axis $+X_2$ of the resultant unit cell, in the $2M_2$ structure along $+Y_2$, and in the $3T$ structure along $-X_1$.

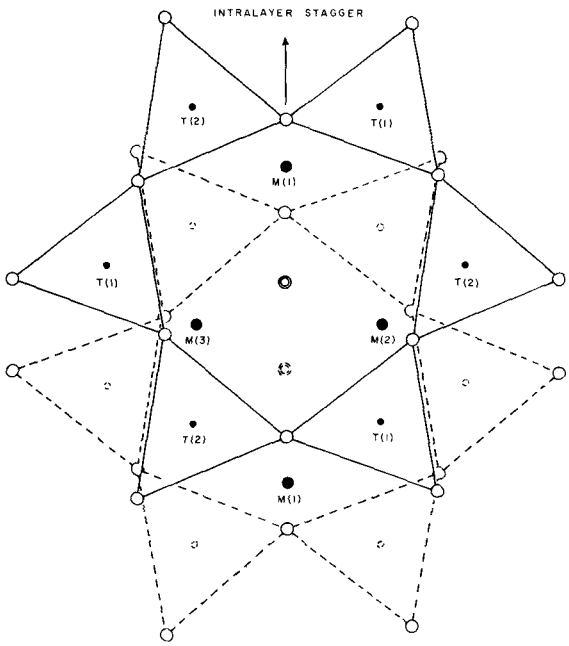

Figure 2. Recommended notation system for tetrahedral and octahedral sites in the first layer of a mica structure. Upper tetrahedral sheet is shown in full line, lower sheet in dashed line.

There already is a consensus among authors that the octahedron with its OH,F groups in the *trans* orientation is to be labeled M(1). In Figure 2 the *cis* octahedron closest to the symmetry plane of the layer and to the right is labeled M(2) in the present system. The *cis* octahedron to the left, if not equivalent by symmetry to M(2), is to be labeled M(3).

Localized sites of ordering

Table 4 summarizes the application of the standard notation system to some of the ordered micas listed in Tables 1 and 3. It is necessary to evaluate each structural type separately. No preferred locus of tetrahedral cation ordering is evident in the $1M$ and $2M_1$ structures, but few examples are available for comparison and only a small degree of ordering has been postulated in some cases. In all four $3T$ structures Al^{IV} is in site T(2), and in the three ordered phengite structures Al^{IV} is also in site T(2). Octahedral cation ordering may or may not be present in the same crystal that shows

https://doi.org/10.1346/CCMN.1984.0320201 Published online by Cambridge University Press

Table 4. Absolute locus of ordering in micas.

Poly-type	Species	Reference	Space group	Al^{IV} site	Oct. site	Local balance	Avoidance imbalance
$1M$	phengite	Sidorenko *et al.* (1975)	$C2$	T(2)	R^{2+} in M(3)	—	Yes
	zinnwaldite	Guggenheim and Bailey (1977)	$C2$	T(1)	Al in M(3)	Yes	—
$2M_1$	phengite	Güven (1971a)	$C2/c$	T(2)	M(2) × 2	—	—
	margarite	Guggenheim and Bailey (1975, 1978)	Cc	T(1) and T(22)	R^{2+} in M(2)	—	Yes
	margarite-bityite	Lin and Guggenheim (1983)	Cc	T(1) and T(22)	M(1) > M(2) = M(3)	—	—
$2M_2$	phengite	Zhoukhlistov *et al.* (1973)	$C2/c$	T(2)	M(2) × 2	—	—
$3T$	muscovite	Güven and Burnham (1967)	$P3_112$	T(2)	R^{2+} in M(2)	—	No
	paragonite	Sidorenko *et al.* (1977)	$P3_112$	T(2)	Al in M(3)	—	Yes
	lepidolite	Brown (1978)	$P3_112$	T(2)	Al in M(3)	No	—
	protolithionite	Pavlishin *et al.* (1981)	$P3_112$	T(2)	Al in M(3)	No	—

tetrahedral cation ordering. Neglecting the usual preference of vacancies and larger cations for octahedral site M(1), no marked tendency exists for M(2) to be larger or smaller than M(3) as a result of ordering. On the basis of these limited data, Al^{IV} tends to localize in site T(2) in phengites, and the sequence of layer stacking tends to influence the localization of tetrahedral cations only in the $3T$ structure. The reason for this influence is not known at present. Verification of any trends for localization of cations will require the results of many more structural refinements of high accuracy than are presently available.

It is not surprising that either the tetrahedral or octahedral cations show little or no preference for specific structural sites when the symmetry is reduced by ordering from that of the parent space group to that of a subgroup, such as in the change from $C2/m$ to $C2$ for the $1M$ structure. In the $1M$ structure tetrahedra T(1) and T(2) would be equivalent to one another in $C2/m$ symmetry, as would octahedra M(2) and M(3), and the selection of specific ordering sites in the higher symmetry where ordering must start should be a matter of random choice at first. It is to be expected that cooperative forces would tend to extend initial randomly scattered ordering "seeds" into larger local domains and that the coalescence of adjacent domains would result in a true single crystal only if there were effective tendencies for ordering into the same specific structural sites in each domain. Favorable crystallization and cooling conditions could aid in this process, as suggested by Soboleva and Mineeva (1981) for phengite-$1M$. It is more likely that adjacent local domains would have different ordering patterns due to the random choice effect and that coalescence of these domains would result in out-of-step relations or twinning that may or may not be discernible from the usual Bragg diffraction spectra. One possible explanation for the lack of observed long-range tetrahedral ordering in the abundant $1M$ phlogopite-biotites and $2M_1$ muscovites is that the ordering for these compositions is entirely in local domains and that the average of all of the domains is long-range tetrahedral disorder as determined by the normal X-ray and electron diffraction techniques (see next section on short-range order). This is equivalent to saying that the energies of all the ordering patterns present in the local domains are about the same, so that no one pattern is predominant. For reasons not yet understood, the $3T$ structure is most conducive to tetrahedral ordering for a variety of compositions, and the phengite composition likewise for a variety of layer stacking arrangements. Phengite ordering may be related to the restricted conditions of low-temperature and high-pressure metamorphism or of hydrothermal solutions under which the specimens studied are believed to have formed. The finding of Rule and Bailey (unpublished) that phengite from the amphibolite facies is disordered also suggests some environmental control.

Table 4 is not specific as to the absolute locus of cations in the $2M_1$ structure when the symmetry is reduced to subgroup Cc. For example, the published atomic coordinates for margarite-$2M_1$ show Al^{IV} to be located in T(1) of the upper tetrahedral sheet of the first layer and in T(22) of the lower tetrahedral sheet (right-hand side of the pseudo symmetry plane) with the phengitic R^{2+} octahedral cations located in site M(2). But if this structure is rotated 180° about the crystallographic Y axis and the origin shifted by $c/2$, the Al^{IV}

https://doi.org/10.1346/CCMN.1984.0320201 Published online by Cambridge University Press

sites would be described as T(2) and T(11) and the octahedral R^{2+} site as M(3) according to the conventions for standard notations adopted above. These two apparently different patterns in fact are equivalent in *Cc* symmetry. Both show avoidance of local charge imbalance, and they would not be equivalent to the two structures that would not show the imbalance effect [e.g., with Al^{IV} in T(1) and T(22) but octahedral R^{2+} in M(3)].

If the two ordering patterns cited above that are equivalent in *Cc* symmetry are adopted at random in different domains of the same crystal, they would have different crystallographic orientations and optical extinction directions and would be described as twinned relative to one another upon coalescence of the domains. Layer silicates with tetrahedral Si:Al ratios near 1:1 have strong ordering tendencies and large resultant domains that are visible under crossed nicols of the petrographic microscope. Complex twinning of this sort that is believed to result from inversion to a lower symmetry is ubiquitous in crystals of margarite, bityite, and ephesite among the micas, and in amesite among the serpentines. Successful crystallographic refinement of these structures requires isolation of a single twin (domain) unit. For smaller domains that are not big enough to give their own X-ray diffraction patterns an average structure will result upon structural refinement.

SHORT-RANGE ORDERING

In addition to ordering over long distances in the crystal, it has been mentioned that it is possible to have ordering in small domains that extend over only a few unit cells. These domains can be seen especially well by transmission electron microscopic techniques. Depending on the details of the ordering patterns and the distribution of domains, such local or short-range ordering may or may not show up during structural refinement as a perturbation of any long-range ordering that may be present. It is quite possible that 100% local order would show up as 0% long-range order. Commonly the domains tend to be antiphase in nature so that the normal diffraction evidence for their presence is cancelled. If the domains are spaced at regular intervals, however, extra diffraction satellite spots will appear, and some conclusions as to the size, distribution, and orientation of the domains can be drawn from the shapes, positions, and intensities of the satellites. Local modulations of the average structure due to the domains will show up as non-Bragg scattering, i.e., diffuse diffracted intensity positioned between the normal Bragg reflections. Such non-Bragg scattering is present in diffraction records of many micas, but its interpretation is controversial.

The lack of long-range order of tetrahedral Si,Al in muscovite-$2M_1$ was mentioned above. Gatineau (1964) interpreted the diffuse non-Bragg scattering in muscovite-$2M_1$ as due to short-range ordering of Al in zigzag chains within the tetrahedral sheet. In a given small domain the direction of chain alignment may be along any one of the three pseudohexagonal X axes of the crystal. Chains of pure Al were said to alternate along the Y direction in partly ordered fashion with chains of pure Si. This interpretation must be viewed with some caution because of the later finding of Kodama *et al.* (1971) that in the local domains the tetrahedral network is distorted in linear waves characterized by alternating rows of tetrahedra of slightly differing dimensions even in the absence of any tetrahedral substitution, e.g., as in pyrophyllite and talc. Further study appears to be required to establish the contributions to the diffuse scattering that may be given by local ordering as well as by such phenomena as the oxygen network distortion, thermal motion, and the presence of dislocation arrays. Similar comments apply to the structures of phlogopite and biotite, for which Gatineau and Méring (1966) observed diffuse scattering very similar to that in muscovite.

Gatineau and Méring (1966) also studied the diffuse X-ray scattering of a lepidolite of unstated structural type. The composition is not given, but by implication is that of polylithionite. Diffuse spots were observed at positions that are satellitic ($\pm a^*/3$) to the positions of certain of the $h + k$ = odd Bragg reflections that are forbidden by C-centering. The spots were interpreted to indicate short-range octahedral ordering of 1Al + 2Li in local domains. The ordering takes the form of rows of pure Al and pure Li aligned along one or the other of the three pseudohexagonal Y axes [01], [31], or [3$\bar{1}$], such that each domain is characterized by only one ordering direction. The ordering is two-dimensional in that the Al rows are spaced regularly within a layer at intervals of $3a/2$ (every third row), but only irregularly between layers. The extent of each domain is small, perhaps due to antiphase relations.

Emphasis in the present paper has been placed on the diffraction method of study of order and disorder. This method requires good quality crystals and considerable expenditure of time for refinement of the structural parameters. Spectroscopic methods, including Mössbauer, infrared, nuclear magnetic resonance (NMR), and Raman, do not have these disadvantages to the same degree and can be effective in determining the distribution of cations and vacancies over the available sites. These methods are sensitive to the local environments of the atoms and therefore can provide information on both long-range and short-range order or disorder. For example, NMR study of phlogopites by Sanz and Stone (1979) has shown that Fe^{2+} tends to be distributed randomly over M(1) and M(2) on a long-range basis. But as the F-content increased local domains were recognized in which Fe^{2+} is concentrated

in association with OH in one type of domain and Mg is concentrated in association with F in another type of domain. In each domain type the cations occupy both M(1) and M(2) sites. Infrared patterns of micas can be interpreted to show the association of one, two, or three nearest-neighbor Fe^{2+} cations around a given OH group, as well as the association of OH with more highly charged cations. These local distributions often average out to long-range disorder as seen by diffraction study.

ACKNOWLEDGMENTS

This study has been supported in part by grant EAR-8106124 from the National Science Foundation, Earth Sciences Division, and in part by grant 13157-AC2-C from the Petroleum Research Fund, administered by the American Chemical Society. The paper has benefited from a review by S. Guggenheim.

REFERENCES

Bailey, S. W. (1975) Cation ordering and pseudosymmetry in later silicates: *Amer. Mineral.* **60,** 175–187.

Bailey, S. W. (1980) Structures of layer silicates: in *Crystal Structures of Clay Minerals and Their X-ray Identification,* G. W. Brindley and G. Brown, eds., Mineralogical Soc., London, 1–124.

Baur, W. H. (1970) Bond length variations and distorted coordination polyhedra in inorganic crystals: *Trans. Amer. Cryst. Assoc.* **6,** 129–155.

Brown, B. E. (1978) The crystal structure of a 3*T* lepidolite: *Amer. Mineral.* **63,** 332–336.

Cruickshank, D. W. J. (1949) The accuracy of electron-density maps in X-ray analysis with special reference to dibenzyl: *Acta Cryst.* **2,** 65–82.

Gatineau, L. (1964) Structure réele de la muscovite. Répartition des substitutions isomorphes: *Bull. Soc. Fr. Minér. Cristallogr.* **87,** 321–355.

Gatineau, L. and Méring, J. (1966) Relations ordre-désordre dans les substitutions isomorphiques des micas: *Bull. Groupe Fr. Argiles* **18,** 67–74.

Guggenheim, S. (1981) Cation ordering in lepidolite: *Amer. Mineral.* **66,** 1221–1232.

Guggenheim, S. and Bailey, S. W. (1975) Refinement of the margarite structure in subgroup symmetry: *Amer. Mineral.* **60,** 1023–1029.

Guggenheim, S. and Bailey, S. W. (1977) The refinement of zinnwaldite-1*M* in subgroup symmetry: *Amer. Mineral.* **62,** 1158–1167.

Guggenheim, S. and Bailey, S. W. (1978) Refinement of the margarite structure in subgroup symmetry: correction, further refinement, and comments: *Amer. Mineral.* **63,** 186–187.

Güven, N. (1971a) The crystal structure of $2M_1$ phengite and $2M_1$ muscovite: *Z. Kristallogr.* **134,** 196–212.

Güven, N. (1971b) Structural factors controlling stacking sequences in dioctahedral micas: *Clays & Clay Minerals* **19,** 159–165.

Güven, N. and Burnham, C. W. (1967) The crystal structure of 3*T* muscovite: *Z. Kristallogr.* **125,** 1–6.

Hazen, R. M. and Burnham, C. W. (1973) The crystal structure of one-layer phlogopite and annite. *Amer. Mineral.* **58,** 889–900.

Kodama, H., Alcover, J. F., Gatineau, L., and Méring, J. (1971) Diffusions anormales (rayons X et éléctrons) dans les phyllosilicates 2-1: in *Structure et Propriétés de Surface des Minéraux Argileux Symposium, Louvain,* 1971, 15–17.

Levillain, C., Maurel, P., and Menil, F. (1981) Mössbauer studies of synthetic and natural micas on the polylithionite-siderophyllite join: *Phys. Chem. Minerals* **7,** 71–76.

Levinson, A. A. (1953) Studies in the mica group: Relationship between polymorphism and composition in the muscovite-lepidolite series: *Amer. Mineral.* **38,** 88–107.

Lin, Cheng-yi and Bailey, S. W. (1984) The crystal structure of paragonite-$2M_1$: *Amer. Mineral.* **69,** (in press).

Lin, J.-C. and Guggenheim, S. (1983) The crystal structure of a Li,Be-rich brittle mica: a dioctahedral-trioctahedral intermediate: *Amer. Mineral.* **68,** 130–142.

Ohta, T., Takeda, H., and Takéuchi, Y. (1982) Mica polytypism: similarities in the crystal structures of coexisting 1*M* and $2M_1$ oxybiotite: *Amer. Mineral.* **67,** 298–310.

Pavlishin, V. I., Semenova, T. F., and Rozhdestvenskaya, I. V. (1981) Protolithionite-3*T*: structure, typomorphism, and practical significance: *Mineralog. Zhurnal* **3,** 47–60 (in Russian).

Sanz, J. and Stone, W. E. E. (1979) NMR study of micas, II. Distribution of Fe^{2+}, F^-, and OH^- in the octahedral sheet of phlogopites: *Amer. Mineral.* **64,** 119–126.

Sartori, F. (1976) The crystal structure of a 1*M* lepidolite: *Tschermaks Mineral. Petrogr. Mitt.* **23,** 65–75.

Sartori, F., Franzini, M., and Merlino, S. (1973) Crystal structure of a $2M_2$ lepidolite: *Acta Crystallogr.* **B29,** 573–578.

Sidorenko, O. V., Zvyagin, B. B., and Soboleva, S. V. (1975) Crystal structure refinement for 1*M* dioctahedral mica: *Kristallografiya* **20,** 332–335 (Engl. transl.).

Sidorenko, O. V., Zvyagin, B. B., and Soboleva, S. V. (1977) The crystal structure of 3*T* paragonite: *Kristallografiya* **22,** 557–560 (Engl. transl.).

Smith, J. V. and Yoder, H. S. (1956) Experimental and theoretical studies of the mica polymorphs: *Mineralog. Mag.* **31,** 209–235.

Soboleva, S. V. and Mineeva, R. M. (1981) Stabilité de différents polytypes de micas dioctaédriques en fonction des potentiels partiels sur les atomes: *Bull. Mineral.* **104,** 223–228.

Swanson, T. H. and Bailey, S. W. (1981) Redetermination of the lepidolite-$2M_1$ structure: *Clays & Clay Minerals* **29,** 81–90.

Takeda, H. and Burnham, C. W. (1969) Fluor-polylithionite: a lithium mica with nearly hexagonal $(Si_2O_5)^{2-}$ ring: *Mineral. Jour.* **6,** 102–109.

Takeda, H., Haga, N., and Sadanaga, R. (1971) Structural investigation of polymorphic transition between $2M_2$-, 1*M*-lepidolite and $2M_1$ muscovite: *Mineral. Jour.* **6,** 203–215.

Takéuchi, Y. and Sadanaga, R. (1966) Structural studies of brittle micas. (I) The structure of xanthophyllite refined: *Mineral. Jour.* **4,** 424–437.

Toraya, H. (1981) Distortions of octahedra and octahedral sheets in 1*M* micas and the relation to their stability: *Z. Kristallogr.* **157,** 173–190.

Toraya, H., Iwai, S., Marumo, F., Daimon, M., and Kondo, R. (1976) The crystal structure of tetrasilicic potassium fluor mica, $KMg_{2.5}Si_4O_{10}F_2$: *Z. Kristallogr.* **144,** 42–52.

Toraya, H., Iwai, S., and Marumo, F. (1977) The crystal structure of taeniolite, $KLiMg_2Si_4O_{10}F_2$: *Z. Kristallogr.* **146,** 73–83.

Toraya, H., Iwai, S., and Marumo, F. (1978) The crystal structure of germanate micas, $KMg_{2.5}Ge_4O_{10}F_2$ and $KLiMg_2Ge_4O_{10}F_2$: *Z. Kristallogr.* **148,** 65–81.

Veblen, D. R. (1983) Exsolution and crystal chemistry of the sodium mica wonesite: *Amer. Mineral.* **68,** 554–565.

Velde, B. (1980) Cell dimensions, polymorph type, and infrared spectra of synthetic white micas: the importance of ordering: *Amer. Mineral.* **65,** 1277–1282.

Zhoukhlistov, A. P., Zvyagin, B. B., Soboleva, S. V., and Fedotov, A. F. (1973) The crystal structure of the dioctahedral mica $2M_1$ determined by high voltage electron diffraction: *Clays & Clay Minerals* **21,** 465–470.

(Received 22 April 1983; accepted 12 August 1983)

Резюме—Длиннопробежному упорядочению тетраэдрических катионов в слюдах благоприятствуют фенгитические составы, порядок $3T$ расположения слоев и тетраэдрически отношения Si:Al близкие 1:1. Считается, что фенгиты политипов $1M$, $2M_1$, и $2M_2$ показывают частично упорядочение тетраэдрических катионов, хотя количества тетраэдрических замещений неболшие и точности их определения не так высоки, как желаемые. $3T$ структуры мусковита, парагонита, лепидолита, протолитионита показывают тетраэдрическое упорядочение также, как $2M_1$ хрупкий маргарит и промежуточные слюды между маргаритом и битиитом. Мусковит $3T$ и маргарит $2M_1$ являются также немного фенгитическими по отношению к их идеальным составам. Примеры упорядочения октаэдрических катионов в слюде более распространены и могут выступать в присутствии катионов различных размеров и зарядов. Размер октаэдрона M(1) со своими OH,F группами с *транс* ориентацией стремится быть больше, чем средняя размеров двух октаэдров в ориентации *цис*, как результат упорядочения катионов и свободных мест. В некоторых образцах упорядочение уменьшало истинную симметрию до подгруппы идеальной пространственной группы. Если результатом упорядочения в симметрии подгруппы являются упорядоченные образцы различных геометрий, но с похожими энергиями в очень маленьких областях, суммарная средняя всех элементарных ячеек может симулировать длиннопробежное неупорядочение. [E.G.]

Resümee—Eine weitreichende Ordnung der tetraedrischen Kationen in Glimmern wird durch eine phengitische Zusammensetzung, durch die $3T$ Stapelungsfolge der Schichten und durch tetraedrische Si:Al-Verhältnisse nahe 1:1 begünstigt. Es heißt, daß Phengite der Polytype $1M$, $2M_1$, und $2M_2$ eine teilweise Ordnung der Tetraederkationen aufweisen, obwohl das Ausmaß der tetraedrischen Substitution klein ist, und die Bestimmungsgenauigkeiten nicht zu groß sind, wie man es sich wünschen würde. Die $3T$ Strukturen von Muskovit, Paragonit, Lepidolith und Protolithionit zeigen tetraedrische Ordnung und ebenso die $2M_1$ Sprödglimmer Margarit und ein Zwischenglied zwischen Margarit und Bityit. Muskovit-$3T$ und Margarit-$2M_1$ sind ebenso leicht phengitisch, vergleichen mit ihren idealen Zusammensetzungen. Beispiele für oktaedrische Kationenordnung in Glimmern sind häufiger. Sie sind zu erwarten, wenn Kationen unterschiedlicher Größe und Ladung vorhanden sind. Das Oktaeder M(1) mit seinen OH,F Gruppen in der *trans*-Stellung tendiert dazu, größer zu sein als der Durchschnitt der beiden *cis*-Oktaeder, infolge der Ordnung von Kationen und Leerstellen. In einigen Proben hat die Ordnung die wahre Symmetrie auf eine Untergruppe der idealen Raumgruppe reduziert. Wenn die Einordnung in eine Untergruppensymmetrie zu einem geordneten Muster von verschiedenen Geometrien aber ähnlichen Energien in sehr kleinen Domänen führt, dann kann der Durchschnitt aus allen Einheitszellen eine weitreichende Unordnung vortäuschen. [U.W.]

Résumé—L'ordonnement à longue échéance de cations tétraèdraux dans des micas est favorisé par des compositions phengitiques, par des séquences d'empilement de couches $3T$ et par des proportions tétraèdrales Si:Al près d'1:1. On dit que des phengites de polytypes $1M$, $2M_1$, et $2M_2$ montrent un ordonnement partiel de cations tetraèdraux, quoique les quantités de substitutions tétraèdrales sont petites et la precision de détermination pas aussi grande qu'on la désirerait. Les structures $3T$ de muscovite, de paragonite, de lepidolite, et de protolithionite montrent un ordonnement tétraèdral, comme le font également les micas cassants margarite et un intermédiaire entre la margarite et la bityite. La muscovite-$3T$ et la margarite-$2M_1$ sont aussi légèrement phengitiques par rapport à leurs compositions idéales. Des exemples d'ordonnement de cations octaèdraux dans des micas sont plus abondants comme l'on s'y attendrait lorsque des cations de taille et de charge différentes sont présents. L'octaèdre M(1) avec ses groupes OH,F dans l'orientation *trans* tend à être plus grand que la moyenne des deux octaèdres *cis*, un résultat de l'ordonnement des cations et des espaces vides. Dans quelques échantillons, l'ordonnement a réduit la symmétrie réelle à un sous-groupe de celle du groupe d'espace idéal. Si l'ordonnement dans la symmétrie de sous-groupe résulte en des modèles de géométrie différente mais d'énergies semblables dans de très petits domaines, la moyenne totale de mailles peut simuler le désordre à longue échéance. [D.J.]

Note added in proof.

Sokolova, C. V., Aleksandrova, V. A., Drits, V. A., and Vairakov, V. V. (1979) Crystal structure of two lithian brittle micas: in *Crystal Chemistry and Structures of Minerals,* Nauka, Moscow, 55–66 (in Russian).

The above reference, which has just come to the author's attention, describes two additional mica structures that are ordered in subgroup symmetry. For ephesite-$1M$: R = 11.5% in $C2$, 284 refl. Mean tet. bonds for $Si_{2.2}Al_{1.8}$: T(1) = 1.609 Å, T(2) = 1.764 Å, $\Delta = 11.0\sigma_\Delta$. Mean oct. bonds for $Al_{1.97}Fe_{0.02}Li_{0.67}Na_{0.10}$: M(1) = 2.128 Å, M(2) = M(3) = 1.927 Å. For bityite-$2M_1$: R = 11.5% in Cc, 450 refl. Mean tet. bonds for $Si_{2.00}Al_{1.29}Be_{0.71}$: T(1) = 1.642 Å, T(2) = 1.710 Å, T(11) = 1.717 Å, T(22) = 1.622 Å, ave. $\Delta = 5.7\sigma_\Delta$. Mean oct. bonds for $Al_{2.00}Li_{0.48}Mg_{0.10}Fe_{0.03}$: M(1) = 2.184 Å, M(2) ≃ M(3) = 1.898 Å.